Phys Chem Minerals (2003) 30: 54 – 58
DOI 10.1007/s00269-002-0289-8

ORIGINAL PAPER

A. Cardelli · G. Cibin · M. Benfatto · S. Della Longa
M. F. Brigatti · A. Marcelli

A crystal-chemical investigation of Cr substitution in muscovite by XANES spectroscopy

Received: 23 May 2002 / Accepted: 6 November 2002

Abstract This work introduces a novel procedure to fit the scattering features of XANES spectra. The procedure was applied and validated on a chromium-containing muscovite for which structural and crystal-chemical characterization is available from literature. The simulation, which involved clusters formed by up to 90 atoms, proved to be effective in representing the Cr local environment, even if the system is characterized by a very low metal content, as demonstrated by the extremely good correspondence with experimental data.

Keywords Cr K-edge · XANES spectroscopy · Chromium-containing muscovite

Introduction

Muscovite [ideally, $^{[12]}K^{[6]}Al_2^{[4]}(Si_3Al)\ O_{10}(OH)_2$], a common rock-forming mineral, can host different cations at tetrahedral and octahedral positions (Brigatti and Guggenheim 2002). Conventional crystallographic methods sometimes proved to be not fully effective in representing the local metal environment in muscovite samples despite its significance as petrogenetic indicator. Information on site occupancy, cation ordering and transition metal oxidation state can thus be difficult to obtain from traditional X-ray diffraction experiments.

The aim of this work is thus to describe Cr local environment (oxidation state, site occupancy and local distortion) in a low Cr-containing system, starting from a novel approach involving the simulation of the multiple-scattering features of XANES spectra deriving from substitution patterns involving tetrahedral, octahedral and interlayer sites.

A. Cardelli · G. Cibin · M. Benfatto · A. Marcelli (✉)
INFN, Laboratori Nazionali di Frascati,
00044 Frascati, Italy
E-mail: marcelli@lnf.infn.it
Fax: +39-06-94032597

S. Della Longa
Dipartimento Medicina Sperimentale, Università L'Aquila,
via Vetoio – 67100 – L' Aquila, Italy,
and INFM – Universita' Roma I,
P.za A. Moro 1, 00185 – Roma, Italy

M. F. Brigatti
Dipartimento di Scienze della Terra,
Universita'degli Studi di Modena e Reggio Emilia,
Largo S. Eufemia 19,
41100 Modena, Italy

Experimental

Sample

Brigatti et al. (2001) performed a crystal-chemical study on the Cr-containing muscovite under investigation, starting from different analytical techniques. This sample is from North Westland glacial moraines (New Zealand) and shows the following composition $^{[12]}(K_{0.857}Ba_{0.044}Na_{0.103})$ $^{[6]}(Al_{1.858}Ti_{0.003}Fe^{2+}_{0.039}Cr^{3+}_{0.062}Mg_{0.081})$ $^{[4]}(Si_{3.110}Al_{0.89})O_{10.166}(OH)_{1.829}Cl_{0.005}$, thus being characterized by moderate homovalent and heterovalent substitutions that involve octahedral, tetrahedral and interlayer positions. Single-crystal structure refinements give tetrahedral mean bond distances [$\langle T–O\rangle = 1.646(1)$ Å for both T1 and T2 tetrahedra] very close to the end-member muscovite [$\langle T1–O\rangle = 1.646(5)$ Å and $\langle T2–O\rangle = 1.647(5)$ Å; Guggenheim et al. 1987]. The mean electron counts for the *cis*-octahedral site (M2), greater than 13, indicate that cations heavier than Al were located at the M2 site. Furthermore, the $\langle M2–O\rangle$ mean bond distance is very close to muscovite [$\langle M2–O\rangle = 1.931(1)$ Å in sample from Westland; $\langle M2–O\rangle = 1.935(5)$ Å in muscovite; Guggenheim et al. 1987]. Unlike muscovite, where the *trans*-octahedral cavity (M1) is completely empty, this sample shows residual areas of positive electron densities in the M1 position, suggesting an M1 partial occupancy. These results suggest a Cr preference for the octahedral sites, but cannot return definite evidence about Cr ordering at the two independent octahedral sites and about the local structural arrangement that the metal imparts to the layer.

XANES spectra

XANES spectra of chromium-containing muscovite were obtained at the GILDA (BM 8) beamline at the European Synchrotron Radiation Facility at Grenoble. Muscovite powder samples were prepared by fine grinding and deposition on a Millipore membrane.

Experiments were performed, using a double-crystal monochromator equipped with Si(311) crystals, at 0.5 eV resolution in fluorescence mode using a 13-element Ge detector. Typical acquisition time was 3 s, and energy calibration was carried out using a reference Cr foil. The experimental data spectra were background-subtracted, normalized at high energy using a standard procedure and averaged. Due to the low concentration, the signal-to-noise ratio obtained at the Cr K edge is about 10^3.

Theoretical method

The XANES analysis was carried out by using a new program, MXAN, which is able to perform a quantitative analysis of the spectra (Benfatto and Della Longa 2001; Della Longa et al. 2001). This method is based on the comparison between the experimental data and several simulations performed by varying selected structural parameters starting from a given geometrical configuration around the absorber atom. The photoabsorption cross-section is calculated using the full multiple-scattering (MS) scheme in the framework of the muffin-tin approximation for the shape of the potential. Muffin-tin radii are calculated on the basis of the Norman criterion with 2% overlapping. Details of the method can be found in Hedin and Lundqvist (1969); Gelatt et al. (1983); Tyson et al. (1992); Benfatto and Della Longa (2001) and Della Longa et al. (2001). In this work the best-fit calculations are made by using a cluster of 89 atoms.

Results and discussion

The bottom curve in Fig. 1 reports the Cr K-edge absorption spectrum obtained on the chromium-containing muscovite from Westland. The spectrum is similar to the ones reported by Brigatti et al. (2001), obtained on Cr-bearing muscovite samples, and exhibits a higher signal-to-noise ratio. This resolution allows the identification of a clear double pre-edge structure (Fig. 1, inset) with relative maximum values at 5998.5 and 5990.5 eV. Two contributions (A and A′) can be observed at the rising edge. They are followed by a double main structure (peaks B and C) with two maximum values at 6008.5 and 6020.2 eV, respectively. The spectrum is characterized by broad features in the intermediate multiple-scattering (IMS) region and almost three contributions can be here identified: D, E and F. Two minor features (G and H) follow at around 6105 and 6135 eV and precede the first main EXAFS oscillation (I) at 6168 eV.

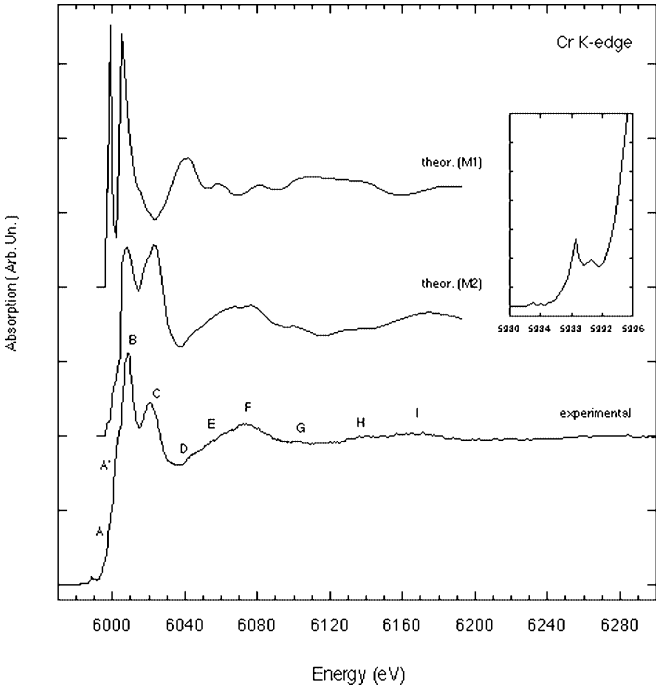

Fig. 1 Comparison between the experimental (*bottom*) Cr K-edge absorption spectrum of chromium-containing muscovite from Westland (NZ) and the theoretical results of the two octahedral clusters: M1 (*top*) and M2 (*middle*). The *inset* enlarges the pre-edge region of the experimental spectrum. The *energy values* refer to the experimental data

XANES data, and particularly the presence of a pre-edge structure, following a transition to *d* empty states in a distorted octahedral entity, support the octahedral coordination of Cr. A previous estimation (Brigatti et al. 2001) determined an upper limit for the presence of Cr in tetrahedral coordination to less than 0.5% of the total chromium content. This value was obtained from a fit procedure of the pre-edge with Gaussian components and from the comparison with the tetrahedrally coordinated model compound $SrCrO_4$. Given the Cr octahedral coordination, a further development involves the identification of the octahedral site at which Cr is preferentially located. An attempt is here made to distinguish between the two possible octahedral sites that could host Cr in muscovite. The *trans*-octahedral (M1) and the *cis*-octahedral (M2) sites, as determined by XRD, are different in topology. In particular, their different mean bond lengths, $\langle$M1–O$\rangle$ and $\langle$M2–O$\rangle$, reflect different electrostatic interactions on neighbouring oxygen atoms [$\langle$M2–O$\rangle = 1.931(1)$ Å; $\langle$M1–O$\rangle = 2.244(1)$ Å]. The M2 site is not only smaller, but also less distorted than the M1 site (octahedral angle variance, $OAV = 109.2^{\circ 2}$ and $58.7^{\circ 2}$ for M1 and M2 site, respectively). Furthermore, in the 2 : 1 layer of dioctahedral micas (space group $C2/c$), each *cis*-octahedral site (M2) is surrounded by three other equivalent *cis*-octahedra and by three empty M1 cavities, whereas the *trans*-octahedral cavity is confined by six *cis*-octahedra, thus accounting for a different topology and different interactions both inside and outside the octahedral sheet (Ferraris and Ivaldi 2002). Following these structural considerations, the Cr K-edge absorption-simulated spectra are significantly different if chromium is set at the M1 or at M2 position. Figure 1 reports the comparison between the simulated spectra assuming for Cr an M1 (top spectra) or M2 (middle spectra) occupancy. More consistent results with experimental data were obtained under the hypothesis of M2 occupancy, whereas when Cr is placed at M1, simulated spectra and experimental data mostly differ in the distance between the two main features (about 7 eV for M1) and for the presence of a sharp contribution ~40 eV above the absorption edge. In this way, both the octahedral

coordination for Cr is confirmed, as supported also by the pre-edge analysis, and the relative occupancy of Cr at M1 site is below the detection limit in Westland muscovite.

Figure 2 reports the effect of an increase in the number of atoms around the absorber on the evolution of the Cr spectral features. An 89-atom cluster, corresponding to a distance of 6.4 Å from the absorber, can be considered as optimal, following the convergence of the total cross-section with respect to the number of atoms. No significant difference in simulated spectra was, in fact, observed moving from 70 to 89 atoms in the cluster. Features E and F are present only in clusters including the potassium cations nearest to the photoabsorber. The interlayer cation is thus the nearest neighbour of the octahedron and it is placed in the tetrahedral cavity at a distance of approximately 5.3 Å from the centre of M2. More quantitative structural information on the Cr local environment can be obtained from the MXAN package, considering only some possible structural deformations induced by Cr over an unperturbed lattice. Figure 3 presents the effects of some structural variations around Cr.

A set of MS simulations was thus performed assuming different displacement modes of the atomic groups in different planes and along different directions. The intensity and energy variations of the spectral features were considered as indicators of the agreement with experimental data and of the most sensitive structural parameters.

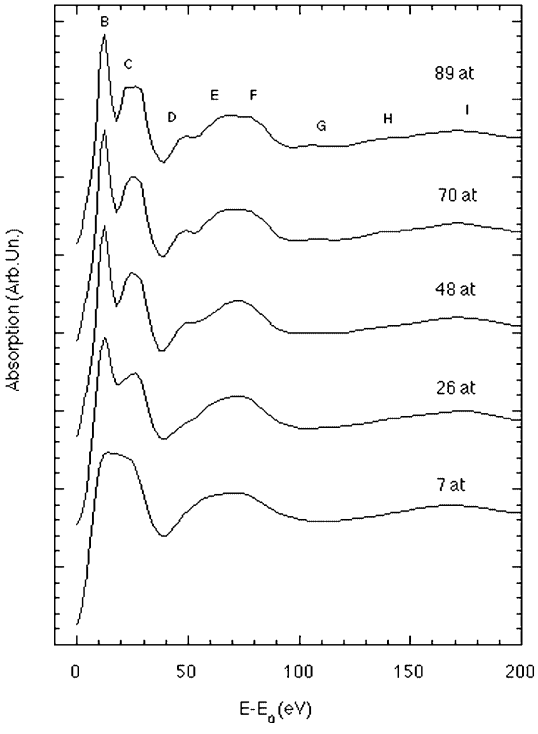

Fig. 2 Theoretical spectra at the Cr K edge for an octahedral M2 surrounding cluster of increasing size from 7 to 89 atoms. The *energy values* refer to the threshold energy E_0

A rigid displacement of the upper and lower octahedral surfaces characterizes the first set of spectra (referred to as [1]). Each octahedral surface is formed by groups of three oxygen atoms along the [001] direction. The induced Cr–O distance variations are correlated to the main oscillation maximum and the relative intensity of the D–E–F features slightly modify together with the B/C height ratio. The second set (referred to as [2]) relates to the effect of the simultaneous radial displacement in the (001) plane of three atom groups, each composed by two near-octahedral O vertices rigidly linked to the Al atom nearest to Cr in the M2 position. Each of these groups is moved in the Cr–Al bond direction. Like the first set, the second set of spectra is characterized by the shift of the I feature, due to the Cr–O distance variation, and by the modification of the weight of the G and H structures. The F peak becomes more evident when the Cr–Al distance increases. The intensity and the position of the main

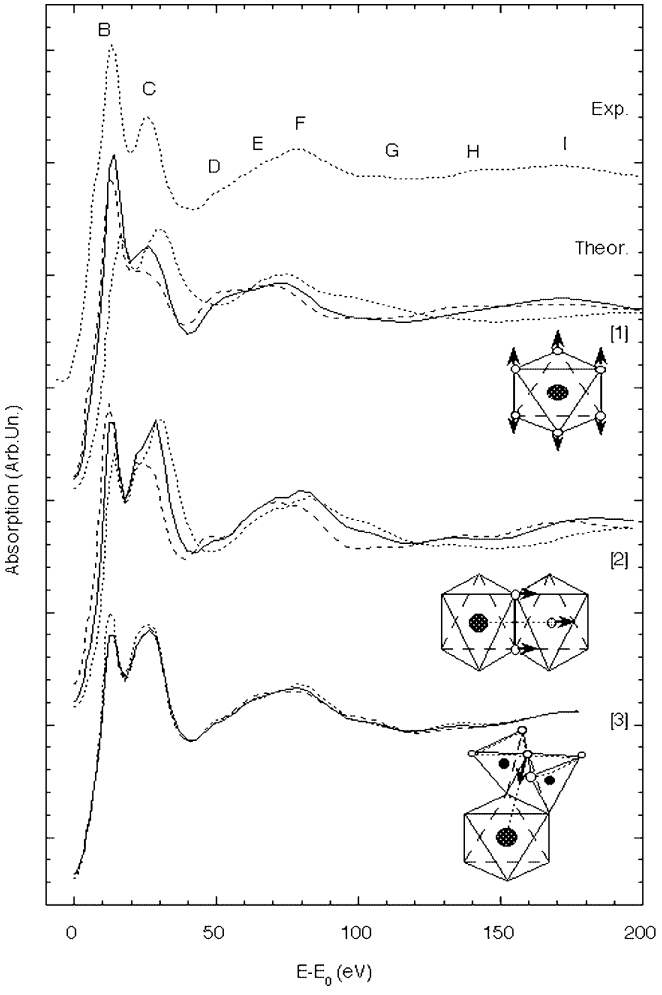

Fig. 3 Effect of several displacement modes of the entities surrounding Cr at M2 site over simulated Cr K-edge spectra. The top curve reports the experimental spectrum. The three others are the simulated spectra referring to displacement modes [*1*], [*2*] and [*3*], as defined in the text. Schematic drawings of the cluster deformation are included. The *energy scale* is the same as in Fig. 2

B and C peaks are strongly influenced by these distortions. The last set of spectra (referred to as [3]) is associated with the movement of the nearest tetrahedra.

The basal oxygen atoms of the four tetrahedra nearest to M2, two below and two above the octahedral sheet, were connected to the Si atoms placed at their centre, thus forming two atomic groups opposite with respect to the octahedral sheet. These groups were moved in the direction defined by the adsorber and by the oxygen atoms shared between the tetrahedra.

This displacement induces only minor spectral changes, mostly involving G and H features that become more separated and stronger with an increase of the Cr–T distance. However, the entire IMS region is weakly affected by this latter distortion. Other structural modifications, like the substitution of Si for Al in the T sites, induce even smaller effects on the spectral features.

The calculation so far presented thus allowed the identification of the parameters to be used in the final fitting procedure of the experimental data. A first fit of the experimental spectrum was performed moving the upper and lower octahedral surfaces in the [001] direction, as described in [1]. This movement is independent of [2] and [3], because the MXAN program allows for separate fitting simulations only when atomic displacements are described in Cartesian or polar coordinates. The minimization procedure converged on a vertical displacement of 0.10 ± 0.01 Å. A new initial configuration was thus derived from this best-fit result and the process was iterated for the two remaining radial movements ([2] and [3]). A MINUIT fit convergence showing an almost diagonal (2 × 2) correlation matrix between the parameters was obtained. The final fit result is reported in Fig. 4 and compared with the reference experimental spectrum. In the lower part of Fig. 4, the absorption spectrum calculated using the initial atomic configuration resulting from the diffraction data is reported for comparison. The agreement between the experimental data and the result of the fitting procedure is very good, in both intensity and position of all the spectral features, confirming the occupancy of Cr at M2. Furthermore, the atomic positions resulting from the fitting procedure show a slight enlargement of the octahedron ($\Delta R = +0.011 \pm 0.001$ Å) in (001) and a reduction of the radial distance of the near tetrahedra ($\Delta R = -0.05 \pm 0.02$ Å). The final radial displacement of the first oxygen shell and of the second shell tetrahedra is reported in Table 1. The relative variation of the distances from the absorber is +3.4 and −2.1%, respectively. The displacement of Al atoms in (001) is +1.2%.The octahedron enlargement is particularly significant when compared to the diffraction data obtained in a Cr-rich mica (Evsyunin et al. 1997), where Cr substitutes for up to 80% of Al in the octahedra. The Cr octahedral average size obtained in the simulation process (1.99 ± 0.01 Å) matches very well the ⟨M2–O⟩ value reported for this Cr-rich mica [1.976(3) Å]. The non-structural parameters fitted in the final atomic configuration are all consistent. The Γ_c value (2.03 eV) representing the energy-independent spectral broadening is in agreement with the core-hole lifetime broadening value, i.e., the natural width of the Cr K atomic level (1.08 eV) (Krause and Oliver 1979), which needs to be combined with the experimental energy resolution. The fitted inelastic losses broadening presents energy threshold and amplitude (respectively 16.58 and 6.66 eV), corresponding to the right plasmon excitation energy and amplitude (Tyson et al. 1992; Benfatto and Della Longa 2001).

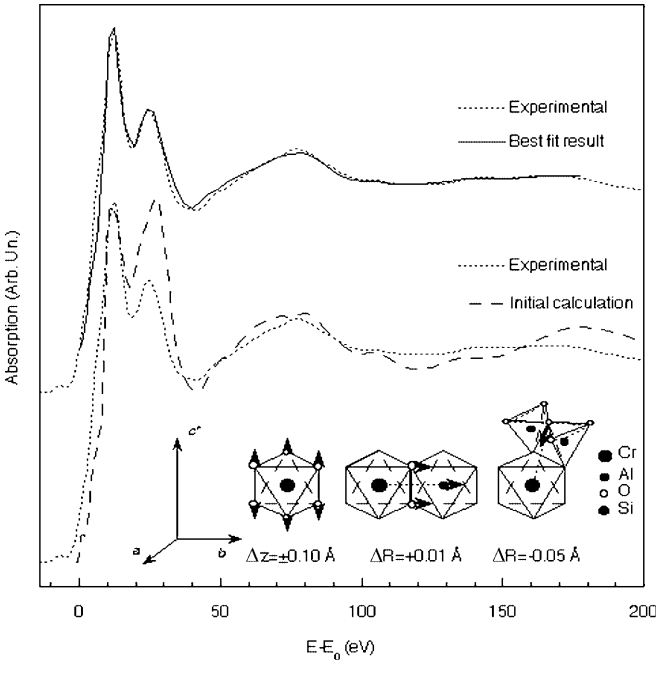

Fig. 4 Comparison between experimental data and the best fit from MXAN procedure. The schematic drawing of the displacement of entities surrounding Cr, which is introduced in the fitting procedure, is included with the distortion parameters obtained as a final result. The *energy scale* is the same as in Fig. 2

Conclusions

Diffraction techniques are a powerful method to characterize natural crystalline systems and, in particular, to

Table 1 Comparison between M2 site bond lengths obtained by X-ray diffraction analysis and XANES fitting results. ⟨Cr–O(tetr)⟩ indicates the distance between Cr and oxygen atoms shared between two nearest tetrahedra considered in the calculation (see Fig. 4 for details)

	XRD	Fit result	Variation
Cr–O31	1.948(1)	2.01(1)	0.06(1)
Cr–O31′	1.924(1)	1.99(1)	0.06(1)
Cr–O32	1.925(1)	1.98(1)	0.06(1)
Cr–O32′	1.946(1)	2.02(1)	0.07(1)
Cr–O4	1.919(1)	1.99(1)	0.07(1)
Cr–O4′	1.921(1)	1.98(1)	0.06(1)
⟨Cr–Al⟩	3.000(1)	3.013(1)	0.012(1)
⟨Cr–O (tetr.)⟩	3.411(1)	3.36(2)	−0.05(2)

determine mean bond distances. However, the local distortions are very difficult to investigate and this task becomes very difficult when the concentration of the atom under investigation is low. X-ray absorption spectroscopy, on the contrary, is sensitive to the local environment and is recognized as a specific method to characterize local coordination and geometrical arrangements, i.e., bond distances and bond angles (Mottana et al. 2002). The improvements achieved in the fitting procedure of the XANES spectra are clearly demonstrated in this paper, where the local geometry was correctly described even in the case of very low substitution and additional potential capabilities never before applied with this spectroscopy are opened for the study of minerals.

The simulation reported in this paper demonstrates that it is possible to improve any previous calculations in terms of both local geometrical description and quantitative determination of the distances. The analysis performed on the spectra of Cr-muscovite under investigation confirms the previous assignment (Brigatti et al. 2001) concerning the octahedral occupancy, but significantly reduces the value of the upper limit occupancy of one of the two possible octahedral site (M1) versus the other (M2). The accuracy of the simulation is excellent and the different possible distortions of the structure were modelled and discussed. In particular, the best fit is obtained when the contribution of the interlayer cation, a basic ingredient of the mica structure is included and distortions of the octahedra are taken into account. In this case, distortions induced by atomic displacements far over the second shell were demonstrated to be substantially negligible.

Acknowledgements Acknowledgment is due to Stefano Colonna and to the GILDA beamline staff for technical assistance during the experimental runs. This work was financially supported by MURST and by the CNR of Italy.

References

Benfatto M, Della Longa S (2001) Geometrical fitting of experimental XANES spectra by a full multiple-scattering procedure. J Synchr Rad 8: 1087–1094

Brigatti MF, Guggenheim S (2002) Mica crystal chemistry and the influence of pressure, temperature, and solid solution on atomistic models. In: Mottana A, Sassi FP, Thompson JB Jr., Guggenheim S (eds) Micas: crystal chemistry and metamorphic petrology. Reviews in Mineralogy and Geochemistry 46: 1–97

Brigatti MF, Galli E, Medici L, Poppi L, Cibin G, Marcelli A, Mottana A (2001) Chromium-containing muscovite: crystal chemistry and XANES spectroscopy. Eur J Mineral 13: 377–389

Della Longa S, Arcovito A, Girasole M, Hazemann JL, Benfatto M (2001) Quantitative analysis of X-ray absorption near-edge structure data by a full multiple scattering procedure: the Fe–CO geometry in photolyzed carbonmonoxy-myoglobin single crystal. Phys Rev Lett 87: 155501–155504

Evsyunin VG, Kashaev AA, Rastsvetaeva RK (1997) Crystal structure of a new representative of Cr micas. Crystallogr Rep 42: 571–574

Ferraris G, Ivaldi G (2002) Structural features of micas. In: Mottana A, Sassi FP, Thompson JB Jr., Guggenheim S (eds) Micas: crystal chemistry and metamorphic petrology. Reviews in Mineralogy and Geochemistry 46: 117–153

Guggenheim S, Chang Y-H, Koster van Groos AF (1987) Muscovite dehydroxylation: high-temperature studies. Am Mineral 72: 537–550

Gelatt CD, Kirkpatrick S, Vecchi MP(1983) Optimization by simulated annealling. Science 220: 671–681

Hedin L, Lundqvist S (1969) Effects of electron–electron and electron–phonon interactions on the one-electron states of solids. In: Seitz F, Turnbull D, Ehrenreich H (eds) Solid state physics, vol. 23. Academic Press, New York, pp 1–15

Krause MO, Oliver JH (1979) Natural widths of atomic K and L levels, K_α X-ray lines and several KLL auger lines. Phys Chem Ref Data 8: 329

Mottana A, Marcelli A, Cibin G, Dyar DM (2002) X-ray absorption spectroscopy of the micas. In: Mottana A, Sassi FP, Thompson JB Jr., Guggenheim S (eds) Micas: crystal chemistry and metamorphic petrology. Reviews in Mineralogy and Geochemistry 46: 371–411

Tyson TA, Hodgson KO, Natoli CR, Benfatto M (1992) General multiple-scattering scheme for the computation and interpretation of X-ray absorption fine structure in atomic clusters with applications to SF_6, $GeCl_4$, and Br_2 molecules. Phys Rev (B) 46: 5997–6019